JOURNAL OF AIRCRAFT
Vol. 40, No. 1, January–February 2003

Robust Aeroelastic Stability Analysis Considering Frequency-Domain Aerodynamic Uncertainty

Dan Borglund*
Kungliga Tekniska Högskolan, SE-100 44 Stockholm, Sweden

The problem of modeling frequency-domain aerodynamic uncertainty for a slender wing structure is investigated. Based on an unsteady lifting-line theory used for the generalized aerodynamic forces, a quite versatile uncertainty description with a clear physical interpretation is proposed. The uncertainty description is easily put in a form suitable for application of the μ framework in robust linear control. Because only frequency response matrices are required for the μ computations, the proposed uncertainty description can be used for robust stability and performance analysis without rational function approximations of the aerodynamic transfer function matrices. The usefulness of the uncertainty description and the methods available for robust aeroelastic stability analysis is demonstrated by performing aeroelastic wind-tunnel experiments.

Introduction

ALTHOUGH the research area of robust stability and performance analysis of aeroservoelastic systems has evolved quite recently,[1] similar considerations for linear control systems have longer traditions.[2] Much progress has been made in the area of robust linear control, and methods such as μ synthesis are considered state of the art for practice. However, the frequency-domain methods practiced in linear control show many similarities with the frequency-domain methods used for linear aeroservoelastic analysis. The important point made by Lind and Brenner[1] is that the stability criterion which paved the way for linear robust control can be directly applied to aeroservoelastic systems as well.

From an aeroservoelastic design point of view, the capability of computing for example robust stability margins is most desirable. As discussed by Kuttenkeuler and Ringertz,[3] there are cases where aeroelastic design optimization of wing structures might actually lead to degraded performance if care is not taken. To avoid such scenarios and take full advantage of the use of optimization methods for design, system uncertainties and deficiencies of the numerical model have to be accounted for in the optimization. The μ approach has provided means to develop robust design schemes, and a very recent example is the work by Moulin et al.,[4] where uncertainty in the inertial properties of an external store load on a wing structure is considered.

If a multidisciplinary analysis is to be used for optimal design, a sufficient accuracy in the disciplinary analyses (such as structures, aerodynamics, and controls) is a prerequisite. However, the usefulness of a robust analysis for design purposes also depends on the availability of a realistic uncertainty description. It is well known that a poor uncertainty description can result in an overly conservative analysis,[1] which is likely to be useless for design purposes. Robust analysis and design must therefore be preceded by the development of realistic and accurate uncertainty descriptions.

Considering aeroservoelastic analysis, the most significant difficulty is the computation of unsteady aerodynamic forces. Because of the complex nature of unsteady aerodynamics, the aerodynamic loads caused by, for example, control surface deflections, are typically associated with some level of inaccuracy. For the purpose of robust optimal design, a useful aeroservoelastic analysis must therefore consider aerodynamic uncertainty. In this study an uncertainty description for frequency-domain slender wing aerodynamics is proposed and demonstrated. The frequency-domain uncertainty description is well suited for the μ framework and is believed to be useful in future studies on robust aeroservoelastic design.

Received 31 March 2002; presented as Paper 2002-1716 at the AIAA/ASME/ASCE/AHS/ASC 43rd Structures, Structural Dynamics, and Materials Conference, Denver, CO, 22–25 April 2002; revision received 24 August 2002; accepted for publication 5 October 2002.

*Research Associate, Department of Aeronautics, Teknikringen 8. Member AIAA.

Frequency-Domain Aeroelasticity

The experimental system on which the present study is based is shown in Fig. 1. A flexible wing with a controllable trailing-edge flap is vertically mounted in a low-speed wind tunnel at Kungliga Tekniska Högskolan. The elastic deformations, in terms of out-of-plane deflections y_j at four different locations on the wing, are monitored by an optical measurement system. The optical system also features a real-time mode, making it possible to use the outputs y_j in a closed-loop feedback system for studies on aeroelastic control.[5,6] In Borglund and Kuttenkeuler[5] a very detailed description of the flexible wing can be found, including planform, structural design, material properties, inertial properties of all main components, and the locations of the optical markers.

The governing equations for small-amplitude motion of a wing structure in low-speed airflow is typically derived by combining a linear finite element structural analysis with a linear unsteady potential flow method for the aerodynamic forces. To obtain an efficient aeroelastic stability or frequency response analysis in the frequency range of interest, the standard procedure is to transform the linear equations of motion to the Laplace domain and introduce modal (or generalized) coordinates corresponding to the M first in-vacuum vibration modeshapes.[3] The Laplace domain equations of motion can then be written in the form

$$[\boldsymbol{I}p^2 + 2\zeta\boldsymbol{\Omega}p + \boldsymbol{\Omega}^2 - q\boldsymbol{A}(pb/u)]\boldsymbol{\eta}(p) = [\boldsymbol{f}p^2 + q\boldsymbol{a}(pb/u)]\delta(p) \tag{1}$$

$$\boldsymbol{y}(p) = \boldsymbol{C}\boldsymbol{\eta}(p) \tag{2}$$

where $\delta(p)$ is the transform of the flap deflection, $\boldsymbol{\eta}(p)$ is the transform of the vector of modal coordinates, and p is the Laplace variable. Normalizing so that the generalized mass of each of the selected vibration modes is one, the generalized mass matrix is the $M \times M$ identity matrix $\boldsymbol{I}$, and the generalized stiffness matrix $\boldsymbol{\Omega}^2$ is diagonal with the squares w_j^2 of the M in-vacuum vibration frequencies on the diagonal. Further, structural damping is approximately accounted for by introducing a uniform modal damping ζ. Based on experimental damping estimates, the value $\zeta = 0.004$ was found to be representative for the frequency range of interest.

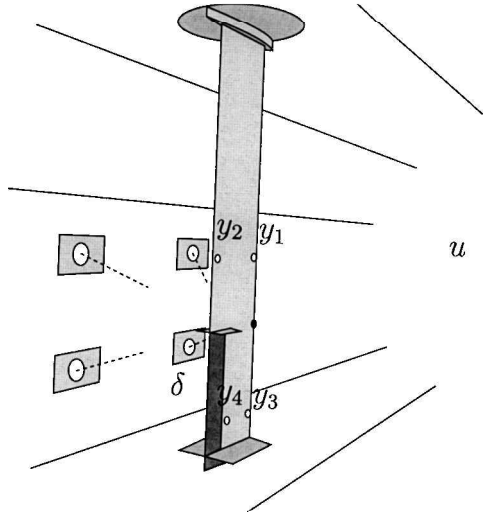

Fig. 1 Schematic layout of the wind-tunnel experiment.

The transfer function matrix $\boldsymbol{A}(pb/u)$ represents the generalized aerodynamic forces in the Laplace domain and depends on the reduced Laplace variable pb/u (Ref. 7). The aerodynamic reference length b is typically chosen as the wing mean semichord, and u is the freestream airspeed. The forces produced by the flap motion are determined by the generalized vector of inertial forces $\boldsymbol{f}$ and the generalized vector of aerodynamic forces $\boldsymbol{a}(pb/u)$. The aerodynamic load magnitude is represented by the freestream dynamic pressure $q = \rho u^2/2$, ρ being the air density. Finally, the vector of measured wing deflections $\boldsymbol{y}(p)$ is related to the modal coordinates through the generalized output matrix $\boldsymbol{C}$.

The aeroelastic frequency response caused by simple harmonic motion of the flap is obtained by evaluating Eqs. (1) and (2) for $p = i\omega$, where ω is the circular frequency of motion. Note that the aerodynamic frequency response matrices depend on the reduced frequency $k = \omega b/u$, which for a given airspeed u and frequency ω is a known parameter. Using a more compact notation, the frequency response of the system can then be written as

$$\boldsymbol{Q}(i\omega, u)\boldsymbol{\eta}(\omega) = \boldsymbol{q}(i\omega, u)\delta(\omega) \tag{3}$$

$$\boldsymbol{y}(\omega) = \boldsymbol{C}\boldsymbol{\eta}(\omega) \tag{4}$$

If there exists a combination of the airspeed u and frequency ω such that the total frequency response matrix $\boldsymbol{Q}(i\omega, u)$ is singular, this means that there exists a nonzero $\boldsymbol{\eta}(\omega)$ such that $\boldsymbol{Q}(i\omega, u)\boldsymbol{\eta}(\omega) = \boldsymbol{0}$. This condition represents self-sustained oscillations of the wing. The lowest airspeed at which this condition can be satisfied by some frequency ω is thus the flutter speed, and the corresponding frequency ω is the flutter frequency.

A well-known method for computation of the flutter boundary is the so-called p-k method,[8] in which the inertial frequency response matrix $\boldsymbol{I}(i\omega)^2$ in $\boldsymbol{Q}(i\omega, u)$ is replaced by the transfer function matrix $\boldsymbol{I}p^2$. The resulting nonlinear eigenvalue problem $\boldsymbol{Q}(p, u)\boldsymbol{\eta}(p) = 0$ is then solved for the approximate poles p (the p-k eigenvalues) for increasing airspeed. The lowest airspeed at which some pole becomes purely imaginary, $p = i\omega$, is the flutter speed. An advantage with this method is that not only the flutter boundary is computed, but also the approximate locations of the poles at subcritical speeds. Another important conclusion is that only the frequency response $\boldsymbol{A}(ik)$ of the unsteady aerodynamic forces is required to compute the flutter boundary.

Previous Work

In the previous study of Borglund and Kuttenkeuler,[5] the equations of motion, Eqs. (1) and (2) for the wing structure in Fig. 1, are obtained by combining linear beam theory with Theodorsen's two-dimensional potential flow theory for the spanwise load distribution[9] and discretizing using beam finite elements. The result of a p-k flutter analysis based on this model is shown in Fig. 2, where the real part of the two dominant p-k eigenvalues are displayed vs airspeed (dashed lines).

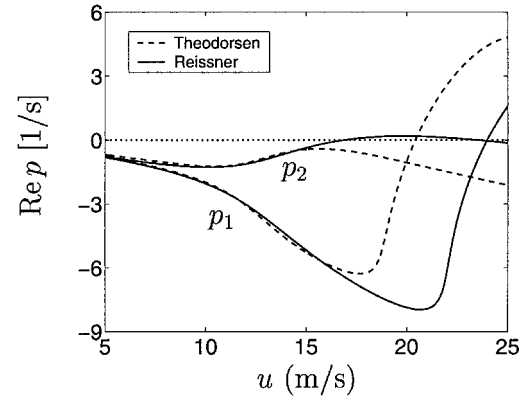

Fig. 2 Real part of the critical p-k eigenvalues vs airspeed u, using the theories by Theodorsen and Reissner.

The wing is predicted to suffer a $f = 3.1$ Hz flutter instability in the first mode when the pole p_1 crosses the stability boundary $Re\, p = 0$ at $u = 20.4$ m/s. However, in the experiment the wing displays a $f = 6.4$ Hz flutter instability in the second mode at $u = 16.0$ m/s, meaning that the pole p_2 actually moves into the unstable region at this speed. Obviously, the model based on Theodorsen's theory is not quite capable of predicting the flutter instability observed in the experiment.

In the work reported in Borglund and Kuttenkeuler[5] and Borglund,[6] the second mode flutter instability was suppressed by active closed-loop control of the flap such that the margin to the stability boundary was increased for the uncertain pole p_2. A semiempirical approach was adopted, where the stability margin was increased step by step until the wing was stabilized in the experiment. By this, the feasibility of the control law design was verified, but the results called for an inclusion of the model discrepancies in the design process. However, even if an appropriate representation of the modeling uncertainties would be available, the p-k framework does not allow for a computation of a robust stability margin.[1]

To apply the results from robust control, the aeroelastic model must be completed by a description of the uncertainties. For the present problem the previous studies have clearly indicated that the fairly simple representation of the unsteady aerodynamic loads (neglecting finite span effects) is the dominant model deficiency. Besides the potential difficulty that the model based on Theodorsen's theory is too poor of a nominal model, which can easily make a robust analysis overly conservative, it is not obvious how to derive a realistic uncertainty description. Therefore, an aerodynamic model based on Reissner's unsteady lifting-line theory for slender wings[9] was developed, which at the same time provided a useful structure for frequency-domain aerodynamic uncertainty.

Lifting-Line Aerodynamics

Based on slender-wing assumptions, Reissner derives a frequency-domain integro-differential equation of the lifting-line type.[9] The equation relates the downwash of wing vibration mode m and the resulting spanwise circulation distribution $\Gamma_m(y, k)$, where $y \in [0, L]$ denotes the spanwise coordinate and L the wing semispan. Reissner proceeds by replacing the unknown $\Gamma_m(y, k)$ by a truncated Fourier expansion

$$\Gamma_m(y, k) = \sum_{n=1}^{N} \gamma_{mn}(k)\varphi_n(y) \tag{5}$$

where the real-valued shape functions $\varphi_n(y)$ satisfy $\varphi_n(L) = 0$ and the first shape function $\varphi_1(y)$ corresponds to an elliptic load distribution. The condition of vanishing circulation at the wing tip is thus identically fulfilled by the expansion. When inserted into the integro-differential equation, a system of equations for the N

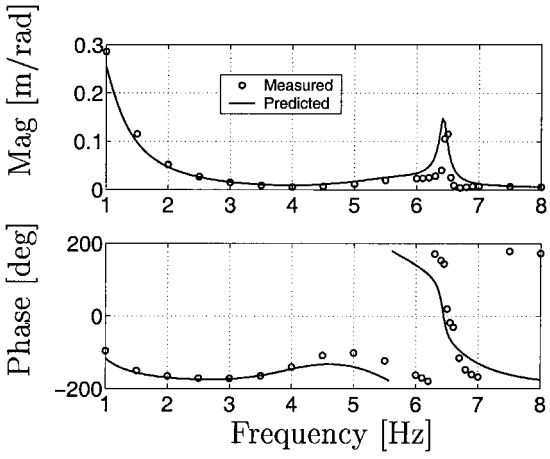

Fig. 3 Bode representation of the measured and predicted frequency response $g_1(i\omega, u)$ at $u = 15.0$ m/s.

Fourier coefficients $\gamma_{mn}(k)$ is formed by evaluating the equation at N different spanwise stations for a fixed reduced frequency k.

The procedure proposed by Reissner was applied to the present problem with a somewhat refined numerical treatment. The first $N = 7$ Fourier coefficients for the $M = 5$ first free vibration modes and the flap mode were computed for a discrete set of reduced frequencies, from which intermediate values are obtained by interpolation. For the purpose of flutter analysis, the aerodynamic loading can usually be modeled with sufficient accuracy using only a few terms (as low as three or four) in the expansion Eq. (5) (Ref. 9). However, the flap mode might require additional terms as a result of the more local variation of the circulation along the span. Finally, the corresponding aerodynamic frequency response matrices $\boldsymbol{A}(ik)$ and $\boldsymbol{a}(ik)$ were derived by computing consistent aerodynamic nodal forces in the wing finite beam element model and introducing modal coordinates.

The result of a *p-k* flutter analysis using the improved aerodynamic model is compared to the preceding model in the graph of Fig. 2 (solid lines). The improvement of the flutter prediction is clear. With the lifting-line aerodynamics the wing is predicted to suffer a $f = 6.3$ Hz flutter instability in the second mode at $u = 16.9$ m/s, which is very close to the experimental values $f = 6.4$ Hz and $u = 16.0$ m/s. Further, the critical speed for the first mode is increased to $u = 24.0$ m/s.

The influence of the flap is also predicted with good accuracy, as can be deduced from the Bode diagram of the open-loop frequency response $g_1(i\omega, u) = y_1(\omega)/\delta(\omega)$ at $u = 15.0$ m/s in Fig. 3. The frequency response functions (FRFs) for the outputs are easily computed by combining Eqs. (3) and (4) and solving for $\boldsymbol{y}(\omega)/\delta(\omega)$. Considering the complexity of the system, the agreement between the predicted and measured magnitude and phase, as well as the resonance frequency, is quite remarkable. The remaining outputs show a similar level of agreement.

As reported in Borglund and Kuttenkeuler,[5] the model based on Theodorsen's results consistently overpredicted the magnitude of the frequency response in Fig. 3 by a factor of approximately two, whereas a similar level of agreement was obtained for the phase angle. Taking the improved flutter prediction into account, the present model is therefore considered to be a more promising nominal model, which is to be completed by an uncertainty description. The improvements also verify that the aerodynamic model was the dominant model deficiency, and it is reasonable to assume that the remaining discrepancies are still caused by aerodynamic uncertainty.

Aerodynamic Uncertainty

Using Reissner's approach for solving the lifting-line integro-differential equation, the resulting aerodynamic frequency response matrices can be written in the form

$$\boldsymbol{A}(ik) = \boldsymbol{A}_0(k) + \sum_{m=1}^{M}\sum_{n=1}^{N} \gamma_{mn}(k)\boldsymbol{A}_{mn}(k) \tag{6}$$

$$\boldsymbol{a}(ik) = \boldsymbol{a}_0(k) + \sum_{n=1}^{M} \gamma_{M+1,n}(k)\boldsymbol{a}_n(k) \tag{7}$$

where $\gamma_{mn}(k)$ are the circulation (or loading) coefficients in the expansion Eq. (5). For a more convenient notation the flap mode is considered as the aerodynamic mode $m = M + 1$. The corresponding matrices $\boldsymbol{A}_{mn}(k)$ thus represent the generalized aerodynamic forces caused by the component $\gamma_{mn}(k)\varphi_n(y)$ of the circulatory load distribution $\Gamma_m(y, k)$ for vibration mode m. Further, the matrix $\boldsymbol{A}_0(k)$ represents the noncirculatory aerodynamic loads. In fact, the noncirculatory loading does not vanish at the wing tip in Reissner's approximation. However, the aerodynamic induction effects associated with the noncirculatory part (which does not produce a wake) appear to be small.[9]

Facing the problem of modeling frequency-domain aerodynamic uncertainty, a crucial observation is that the circulatory part of the generalized aerodynamic loads is completely determined by the coefficients $\gamma_{mn}(k)$. For example, $\gamma_{11}(k)$ represents the magnitude and phase shift of the purely elliptical component of the aerodynamic load distribution for the first free vibration modeshape. Assuming that the true loading can be represented by Eqs. (6) and (7) for some coefficients $\tilde{\gamma}_{mn}(k)$ and that the nominal coefficients $\gamma_{mn}(k)$ are close to $\tilde{\gamma}_{mn}(k)$, a straightforward structure for the aerodynamic uncertainty is obtained by writing

$$\tilde{\gamma}_{mn}(k) = \gamma_{mn}(k)[1 + \alpha(k)w_{mn}(k)\delta_{mn}] \tag{8}$$

where the norm-bounded relative uncertainties in the coefficients $\gamma_{mn}(k)$ are scaled such that $\alpha(k)$ is the maximum upper bound, $0 < w_{mn}(k) \le 1$ are the scaled upper bounds, and the complex-valued uncertain parameters δ_{mn} have $|\delta_{mn}| \le 1$. This means that all weights $w_{mn}(k) = 1$ if all coefficients $\gamma_{mn}(k)$ have the same upper bound on the relative uncertainty. Not to get an excessively large uncertainty description, it might be sufficient to model only the most significant coefficients as uncertain. This will be discussed further in the section on model validation. The model including aerodynamic uncertainty is obtained by simply using $\tilde{\gamma}_{mn}$ instead of γ_{mn} for the uncertain coefficients. The uncertain frequency response matrices can then be written as

$$\tilde{\boldsymbol{A}}(ik) = \boldsymbol{A}(ik) + \alpha(k)\sum_{m}\sum_{n} \delta_{mn}w_{mn}(k)\gamma_{mn}(k)\boldsymbol{A}_{mn}(k) \tag{9}$$

$$\tilde{\boldsymbol{a}}(ik) = \boldsymbol{a}(ik) + \alpha(k)\sum_{n} \delta_{M+1,n}w_{M+1,n}(k)\gamma_{M+1,n}(k)\boldsymbol{a}_n(k) \tag{10}$$

where $\boldsymbol{A}(ik)$ and $\boldsymbol{a}(ik)$ are the nominal matrices in Eqs. (6) and (7) and the summations are taken over the uncertain coefficients.

The frequency-domain aerodynamic uncertainty represented by Eqs. (9) and (10) is quite versatile and has a clear physical interpretation. Different values of the uncertain parameters δ_{mn} correspond to a variation of the magnitude and phase shift, as well as the shape of the aerodynamic loading. With the proposed uncertainty description, the uncertain contribution to the loading will not affect the condition of vanishing circulation at the wing tip.

If $\boldsymbol{A}(ik)$ and $\boldsymbol{a}(ik)$ are replaced by $\tilde{\boldsymbol{A}}(ik)$ and $\tilde{\boldsymbol{a}}(ik)$ in Eq. (3), giving

$$[\boldsymbol{I}(i\omega)^2 + 2\zeta\boldsymbol{\Omega}i\omega + \boldsymbol{\Omega}^2 - q\tilde{\boldsymbol{A}}(i\omega b/u)]\boldsymbol{\eta}(\omega) = [\boldsymbol{f}(i\omega)^2 + q\tilde{\boldsymbol{a}}(i\omega b/u)]\delta(\omega) \tag{11}$$

it is now assumed that the true frequency response can be generated by the uncertain system Eq. (11) for some uncertainty represented by the set defined in Eq. (8).

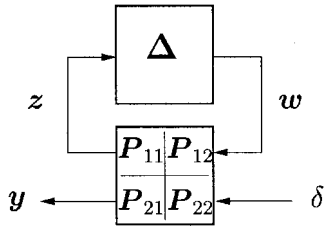

Fig. 4 Uncertain system in the form of a linear fractional transformation.

Model Validation

With the aerodynamic uncertainty description at hand, the μ framework in robust linear control allows for both an estimation of the amount of uncertainty present in the model and a subsequent robust stability analysis.[1] To use these methods, the aeroelastic system (or plant) defined by Eqs. (11) and (4) is written in the form of the linear fractional transformation illustrated in Fig. 4. For the present problem this is accomplished by introducing the signals

$$\boldsymbol{w}_{mn}(\omega) = \delta_{mn}\boldsymbol{z}_{mn}(\omega) \tag{12}$$

where $\boldsymbol{z}_{mn}(\omega)$ denotes the input signals to the uncertain parameter δ_{mn} and $\boldsymbol{w}_{mn}(\omega)$ denotes the uncertain output signals. Based on the system frequency response Eqs. (11) and (4), it is then a straightforward matter to derive the frequency response matrices from each of the plant input signals $\boldsymbol{w}_{mn}(\omega)$ and $\delta(\omega)$ to each of the plant output signals $\boldsymbol{z}_{mn}(\omega)$ and $\boldsymbol{y}(\omega)$. For this problem the normalized uncertainty matrix $\boldsymbol{\Delta}$ is diagonal with the blocks $\delta_{mn}\boldsymbol{I}_{M\times M}$ on the diagonal. In particular it can be noted that $\|\boldsymbol{\Delta}\|_\infty \le 1$ and that the partition $\boldsymbol{P}_{22}(i\omega, u)$ is the nominal frequency response matrix between $\delta(\omega)$ and $\boldsymbol{y}(\omega)$ in the absence of uncertainty. With the scaling used in Eq. (8), $\alpha(k)$ is the upper bound on the 2-norm (the maximum singular value) of the nonscaled uncertainty matrix with the blocks $\alpha(k)w_{mn}(k)\delta_{mn}\boldsymbol{I}_{M\times M}$ on the diagonal.

As suggested in Lind and Brenner,[1] the μ validation test proposed in Kumar and Balas[10] is used to estimate the amount of uncertainty present in the model. At this point it should be noted that the standard μ framework is based on the Small Gain Theorem for rational transfer function matrices,[1] whereas the aerodynamic transfer function matrices underlying Eq. (1) have a nonrational dependence on the Laplace variable.[7] Consequently, if rational function approximations are used for the aerodynamic transfer function matrices[1,4,11] the standard μ framework is applicable. It is however proposed that based on a more general Small Gain Theorem[12] the very same numerical procedures for computation of upper and lower bounds on the structured singular value μ can be applied to the true frequency response matrices of linear aeroservoelastic systems.

Consider now the single-input/single-output (SISO) FRF $g_j(i\omega, u)$ between $\delta(\omega)$ and the output $y_j(\omega)$. Recall for example the Bode diagram of $g_1(i\omega, u)$ in Fig. 3. For each value of the frequency used in the experiment, there is an experimental FRF $g_j^*(i\omega, u)$ and a corresponding nominal prediction $g_j(i\omega, u)$. As shown in greater detail in Kumar and Balas,[10] the uncertain plant with $\|\boldsymbol{\Delta}\|_\infty \le 1$ can match the experimental data identically for an uncertainty norm $\alpha(k)$ if the structured singular value

$$\mu_{\text{val}}(\omega, u) = \mu\left(\boldsymbol{P}_{11} - \boldsymbol{P}_{12}\left(P_{22} - g_j^*\right)^{-1}\boldsymbol{P}_{21}\right) \ge 1 \tag{13}$$

Here, the plant partitions are those corresponding to the considered single output, meaning for example that $P_{22}(i\omega, u)$ is the nominal SISO FRF $g_j(i\omega, u)$. Further, if $\mu_{\text{val}}(\omega, u) \ge 1$ the uncertain model will still validate the data if the norm $\alpha(k)$ is reduced by a factor $\mu_{\text{val}}(\omega, u)$. Hence, the minimum norm of the uncertainty required to validate the experimental data can be computed, which is very desirable in order not to make the subsequent robust stability analysis overly conservative.

The described approach is applied to the present problem using the μ toolbox[13] in MATLAB®. The first problem encountered is to decide which parameters should be modeled as uncertain. There are $R = (M+1)\times N = 42$ coefficients $\gamma_{mn}(k)$ in total for the present problem, which, if all were assumed uncertain, would give an $(R\times M)\times(R\times M) = 210\times 210$ uncertainty matrix $\boldsymbol{\Delta}$. To avoid unnecessary conservatism and reduce computational effort, it is therefore desirable to include only the most significant coefficients representing the likely uncertainty mechanism. Numerical experiments clearly reveal that this selection process can be motivated on physical grounds. It appears that a good rule to obtain a representative reduced size uncertainty model is to select the first few coefficients corresponding to the mode shapes dominating the motion pattern in the frequency range of interest.

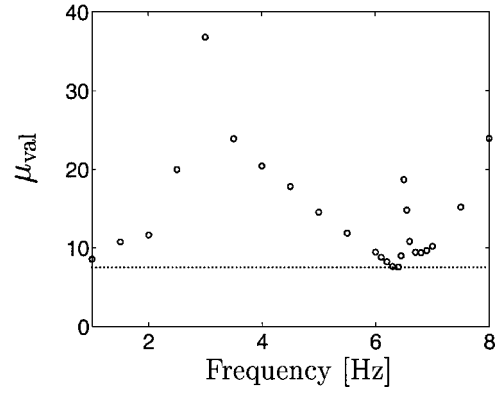

Fig. 5 Model validation at $u = 15$ m/s based on the measured frequency response data in Fig. 3. The horizontal line indicates the minimum value $\mu_{\text{val}}(\omega, u) = 7.5$.

The results from the frequency response and p-k flutter analyses suggest that the aerodynamic loading for the three first vibration mode shapes and the flap mode should be modeled as uncertain for the present system. Selecting the three first coefficients of these modes results in 12 uncertain parameters δ_{mn} and a 60×60 uncertainty matrix $\boldsymbol{\Delta}$. The model is first validated against the FRF data in Fig. 3 using the weights $w_{mn}(k) = 1$ and uncertainty norm $\alpha(k) = 1$. Computing the lower bound on the corresponding $\mu_{\text{val}}(\omega, u)$ gives the result presented in the graph of Fig. 5. The model will still be validated for all experimental data points if the uncertainty norm is reduced by a factor 7.5. It is thus sufficient to use the norm $\alpha(k) = 1/7.5 \approx 0.13$. Somewhat loosely, the result can be interpreted as if a 13% uncertainty in the unsteady aerodynamic loads is required to validate the experimental data. The results for the remaining outputs closely resemble those presented in Figs. 3 and 5 for the first output, and the constant norm $\alpha(k) = 0.13$ is assumed to be representative in the airspeed range of interest.

Note the correlation between the μ validation in Fig. 5 and the FRF comparison in Fig. 3. A higher value of $\mu_{\text{val}}(\omega, u)$ means that less uncertainty is required to make up for the discrepancy between the experimental and nominally predicted FRFs. Consequently, a higher value of $\mu_{\text{val}}(\omega, u)$ in Fig. 5 is expected at those frequencies where the FRFs are close in Fig. 3. This is exactly what is observed, and the physical interpretation of the μ validation is quite clear in this case.

Using an uncertainty description with the same relative uncertainty $\alpha(k)w_m(k)\delta_m$ in the coefficients $\gamma_{mn}(k)$, $n = 1, \ldots, N$ corresponds to a model with an uncertain modal participation in the circulatory loading. With this structure only one uncertain coefficient δ_m per considered mode results, but the capability of varying the shape of the aerodynamic load distributions is lost. For the present problem a 20×20 uncertainty matrix results when using the more restricted structure, but an approximately 15% increase of the uncertainty norm is required to validate the model. This indicates that including the shape of the modal loading in the uncertainty description makes a difference and that the more simple structure can be useful. In this case it is possible that the more general uncertainty description, to some extent, compensates for the effect of the vertical plates located close to the wing tip (see Fig. 1).

Robust Stability Analysis

Provided that the nominal system is stable at a particular airspeed u (which is true for airspeeds below the nominal flutter speed

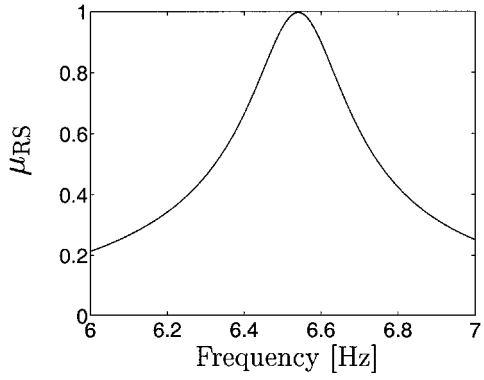

Fig. 6 Structured singular value $\mu_{RS}(\omega, u)$ vs frequency at the airspeed u = 13.5 m/s.

$u = 16.9$ m/s), the wing is robustly stable subject to the aerodynamic uncertainty if

$$\mu_{RS}(\omega, u) = \mu[\boldsymbol{P}_{11}(i\omega, u)] < 1 \tag{14}$$

for all frequencies $w > 0$ (Ref. 1). The robust flutter speed is now computed by considering a discrete set of frequencies ω_j in the frequency range of interest and increasing the airspeed u until some $\mu_{RS}(\omega_j, u) = 1$. In Fig. 6 the upper bound on $\mu_{RS}(\omega, u)$ is shown vs frequency at $u = 13.5$ m/s. At this speed $\mu_{RS}(\omega, u)$ just touches the stability boundary $\mu_{RS}(\omega, u) = 1$, and increasing the speed results in $\mu_{RS}(\omega, u) > 1$ for some frequency range. Consequently, the result of the robust stability analysis is that a flutter instability in the 6.5-Hz range can result from $u = 13.5$ m/s and higher.

At the experimental flutter speed $u = 16.0$ m/s, the flutter frequency $f = 6.4$ Hz is part of the frequency range in which $\mu_{RS}(\omega, u) > 1$, and the flutter instability observed in the experiment is one of the possible outcomes predicted by the robust stability analysis. In this case the robust stability analysis is expected to be somewhat conservative. This is because the uncertainty associated with the flap mode affects the FRF data used for the model validation (and might hence increase the uncertainty norm required to validate the data), but not the open-loop stability of the wing. Using the weights $w_{mn}(k) = 1$ for the flap mode and the vibration modes means that they are assumed to have the same relative uncertainty. However, it is likely that the flap mode is more uncertain than the vibration modes, which can be enforced by using values $w_{mn}(k) < 1$ for the vibration modes. This would however require additional experiments in order to determine the proper weighting. Finally, it must also be emphasized that no uncertainty in the experimental data has been considered, which might be necessary in the general case.

Conclusions

The problem of modeling frequency-domain aerodynamic uncertainty for slender-wing structures has been investigated. Using Reissner's unsteady lifting-line theory for the generalized unsteady aerodynamic forces, a quite versatile uncertainty description with a clear physical interpretation was proposed. With this approach the aerodynamic uncertainty was represented by uncertain coefficients in a Fourier expansion of the spanwise aerodynamic loading for each vibration modeshape. To avoid making the uncertainty description excessively large, the proposal to model only a subset of the coefficients as uncertain was made. It was suggested to select the first few Fourier coefficients corresponding to the mode shapes dominating the motion pattern in the frequency range of interest.

It is also shown that a somewhat simplified structure of the uncertainty can be interpreted in terms of a model with uncertain aerodynamic modal participation. This simplified uncertainty description is not dependent on the method used for computing the aerodynamic frequency response matrices, is not restricted to slender-wing aerodynamics, and requires a minimum number of uncertain parameters.

Because only the aerodynamic frequency response matrices are required for the μ computations, the proposed frequency-domain uncertainty description can be used for robust stability and performance analysis without rational function approximations of the aerodynamic transfer function matrices. An advantage with this approach is that potential modeling errors introduced when using rational function approximations are avoided.

The computational cost using the frequency-domain approach is comparable to that of a rational function approach because the rather expensive computations of the aerodynamic frequency response matrices are required in both cases. Regarding the robust flutter analysis, the main difference is that the aerodynamic forces at a specific frequency are obtained by interpolation in the frequency-domain approach (similar to a p-k flutter analysis), whereas a rational function approach benefits from an explicit dependence on frequency.

The proposed uncertainty description is applied to a slender-wing-type wind-tunnel model in low-speed airflow. For this case it is possible to validate the uncertain model against experimental frequency response data, and a subsequent robust stability analysis succeeds in predicting the experimental flutter instability. These results indicate that the model of the unsteady aerodynamics is the dominant model deficiency and that the proposed uncertainty description for frequency-domain aerodynamic uncertainty is useful in practice.

Acknowledgment

The author gratefully acknowledges the National Program for Aeronautics Research (NFFP) for its financial support.

References

[1]Lind, R., and Brenner, M., *Robust Aeroservoelastic Stability Analysis*, Springer-Verlag, London, 1999, pp. 1–5, 11, 12, 21, 22, 91–93, 99–105.

[2]Zhou, K., Doyle, J. C., and Glover, K., *Robust and Optimal Control*, Prentice–Hall, Upper Saddle River, NJ, 1996, pp. 1–5.

[3]Kuttenkeuler, J., and Ringertz, U. T., "Aeroelastic Design Optimization with Experimental Verification," *Journal of Aircraft*, Vol. 35, No. 3, 1998, pp. 505–507.

[4]Moulin, B., Idan, M., and Karpel, M., "Aeroservoelastic Structural and Control Optimization Using Robust Design Schemes," *Journal of Guidance, Control, and Dynamics*, Vol. 25, No. 1, 2002, pp. 152–159.

[5]Borglund, D., and Kuttenkeuler, J., "Active Wing Flutter Suppression Using a Trailing Edge Flap," *Journal of Fluids and Structures*, Vol. 16, No. 3, 2002, pp. 271–294.

[6]Borglund, D., "Aeroservoelastic Design Optimization with Experimental Verification," *Journal of Aircraft*, Vol. 38, No. 5, 2001, pp. 958–961.

[7]Stark, V. J., "General Equations of Motion for an Elastic Wing and Method of Solution," *AIAA Journal*, Vol. 22, No. 8, 1984, pp. 1146–1153.

[8]Bäck, P., and Ringertz, U. T., "On the Convergence of Methods for Nonlinear Eigenvalue Problems," *AIAA Journal*, Vol. 35, No. 6, 1997, pp. 1084–1087.

[9]Bisplinghoff, R. L., Ashley, H., and Halfman, R. L., *Aeroelasticity*, Dover, New York, 1996, pp. 251–281, 380–394.

[10]Kumar, A., and Balas, G. J., "An Approach to Model Validation in the μ Framework," *Proceedings of the American Control Conference*, 1994, pp. 3021–3026.

[11]Lind, R., "Match-Point Solutions for Robust Flutter Analysis," *Journal of Aircraft*, Vol. 39, No. 1, 2002, pp. 91–99.

[12]Green, M., and Limebeer, D. J. N., *Linear Robust Control*, Prentice–Hall, Upper Saddle River, NJ, 1995, pp. 96–98.

[13]Balas, G. J., Doyle, J. C., Glover, K., Packard, A., and Smith, R., *μ-Analysis and Synthesis Toolbox User's Guide*, Math Works, Natick, MA, 1996.